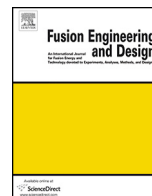




Contents lists available at ScienceDirect

## Fusion Engineering and Design

journal homepage: [www.elsevier.com/locate/fusengdes](http://www.elsevier.com/locate/fusengdes)



# Plasma density control in real-time on the COMPASS tokamak

F. Janky<sup>a,b,\*</sup>, M. Hron<sup>a</sup>, J. Havlicek<sup>a,b</sup>, M. Varavin<sup>a</sup>, F. Zacek<sup>a</sup>, J. Seidl<sup>a</sup>,  
R. Panek<sup>a</sup>, COMPASS Team

<sup>a</sup> Institute of Plasma Physics AS CR, v.v.i., Association EURATOM/IPP.CR, Za Slovankou 3, 182 00 Praha 8, Czech Republic

<sup>b</sup> Department of Surface and Plasma Science, Faculty of Mathematics and Physics, Charles University in Prague, V Holešovičkách 2, 180 00 Praha 8, Czech Republic

### HIGHLIGHTS

- We fitted length of the chord of the interferometry crossing plasma in the different plasma scenarios.
- We add correction to the actual length of the chord of the interferometry according to plasma shape and position in real-time code.
- We used this correction to control plasma density in real-time.

### ARTICLE INFO

#### Article history:

Received 5 October 2014  
Received in revised form 14 April 2015  
Accepted 29 April 2015  
Available online xxx

#### PACS:

52.55.Fa

#### Keywords:

COMPASS tokamak  
Real-time control  
Density control  
MARTE  
Interferometer  
Stickiness of the valve

### ABSTRACT

The electron density on COMPASS is measured using 2 mm microwave interferometer. Interferometer signal is used as an input for the feedback control loop, running under the MARTE real-time framework. Two different threads are used to calculate (fast 50  $\mu$ s thread) and to control (slow 500  $\mu$ s thread) the electron density. The interferometer measures a line averaged density along a measurement chord.

This paper describes an approach to control the line-averaged electron density in a real-time loop, using a correction to the real plasma shape, the plasma position, and non-linear effects of the electron density measurement at high densities.

Newly developed real-time electron density control give COMPASS the chance to control the electron density more accurately which is essential for parametric scans for diagnosticians, for physics experiments and also for achieving plasma scenarios with H-mode.

© 2015 EURATOM/IPP.CR. Published by Elsevier B.V. All rights reserved.

## 1. Introduction

The control of electron density plays an important role in the tokamak operation. The density in a tokamak is influenced by plasma confinement, interaction of the plasma with the wall and the wall conditions in general, active gas feeding, and pumping. Among these, a prospective actuator for electron density control is the gas feeding: pellets, gas injection, and Neutral Beam Injection (NBI). On the other hand, the control of the plasma confinement, plasma-wall interaction, and wall conditions cannot be

used directly for density feedback since these tools either change the discharge scenario or cannot be controlled on the time scale of the COMPASS discharges. Similarly, the pumping speed is a given steady-state quantity which cannot be significantly changed.

Due to its size, COMPASS [1] does not use (and need) the pellet injection to feed the core plasma by the working gas. The NBI [2] power typically brings the COMPASS plasma to the H-mode [3] and then the density rapidly increases and can be controlled only by changing the discharge scenario, particularly by changing the ELM types. Therefore, the most suitable actuator for density control on COMPASS remains the gas injection.

In this paper, we describe the electron density measurement and available control tools (Section 2), the real-time data evaluation and control (Section 3), and finally we present the calibration and results (Section 4).

\* Corresponding author at: Max-Planck-Institut für Plasmaphysik, Boltzmannstr. 2, 85748 Garching, Germany. Tel.: +49 89 3299 1327.  
E-mail address: [filip.janky.work@gmail.com](mailto:filip.janky.work@gmail.com) (F. Janky).

## 2. Electron density measurement and control

COMPASS uses interferometer [4,5] operating with 2 mm electromagnetic wave using two near frequencies 139.3 and 140 GHz. A phase shift that appears between the both waves passing through the plasma along the same chord corresponds to the electron density. This phase shift is processed by measuring circuits, which have a voltage output giving a linear function of the phase shift. Whenever the electron density increases, phase shift increases too.

### 2.1. Influence of the plasma shape and the plasma position on the electron density

The interferometry diagnostic measures the electron density as a line integrated quantity along the chord passing through the plasma. This signal is normalised to the standard circular shape with diameter 0.4 m and then stored in COMPASS Database (CDB) [6] or used as a measured signal for feedback controller. Therefore, when the plasma shape is changed from circular to elongated D-shaped plasma [7] and/or the radial or vertical plasma position is moved [8], the path of the interferometer chord through the plasma changes as well as the line integrated density measured along this chord. Due to these effects, the measured density has to be corrected accordingly. Several different discharge scenarios when shape and vertical and horizontal positions were changing were chosen. Then least square fitting method was used to calculate coefficients offline for these scenarios and results were compared with the EFIT reconstruction. Correction to the interferometry chord length according to the plasma position and the plasma shape is calculated according to Eq. (1).

$$n_{cor} = \frac{n_0}{\left( \sum_{i=1}^{n=5} c_i \cdot \left( \frac{I_{SF}}{I_{pl}} \right)^i + c_R \cdot R + c_Z \cdot Z + c_C \right)} \cdot 0.4 \quad (1)$$

where  $n_{cor}$  is the corrected density according to plasma shape,  $n_0$  is measured density,  $I_{SF}$  is current driven in the shaping field coils and  $I_{pl}$  is plasma current,  $R$  is radial plasma position, and  $Z$  is vertical plasma position.  $c_i$ ,  $c_R$ ,  $c_Z$ ,  $c_C$  are multiplying constants calculated from the fitting.

### 2.2. Correction to the interferometer non-linearity

The interferometer can measure density up to the critical density of  $n_{crit} = 24.08 \times 10^{19} \text{ m}^{-3}$ . However, if the electron density somewhere inside the plasma becomes not negligible compared to the critical density (i.e. the plasma frequency becomes comparable to the probing wave frequency), the measured phase shift does not increase linearly with the increasing averaged density anymore, but faster. In an extreme case, if the linearised form is used, even density value higher than the critical one can be evaluated (clearly incorrect from the physics point of view). It is evident that the effect of non-linearity must be taken into account, if the density exceeds value of about 20% of the critical one (which is a common case of the COMPASS tokamak).

Moreover, the problem is still more complex taking into account the fact that plasma is not homogeneous. As a consequence the local non-linear enhancement of the phase shift is radially dependent and the measured phase shift averaged along the radius is, therefore, not only function of the average density but also function of a density profile.

To estimate the influence of the non-linearity effect on the phase shift in the case of an inhomogeneous plasma, the real (i.e. taking into account non-linearity) local values of the phase shift have been modelled. The phase shift was modelled for homogeneous plasma and for five axially symmetric parabolic density profiles

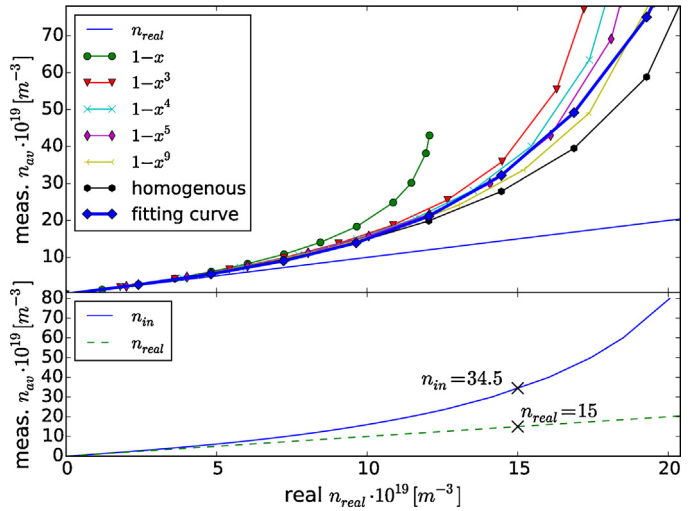


**Fig. 1.** Top: Different conversions between real densities and measured densities assuming different density profiles. Bottom: Conversion between real density and measured density. Dashed line shows density when non-linearity is considered. Example values for the case of  $n_{real} = 15$  are shown.

$n = n_0 \cdot (1 - (r/a)^p)$  ( $p = 1$  – triangle,  $p = 3, 4, 5$  and  $p = 9$  – approaching the homogeneous one) and numerically integrated along the radius  $r$ . For each profile we increased the central density  $n_0$  step by step from zero to the critical one (till probing wave cut-off was reached). The incorrectly evaluated averaged densities  $n_{in}$  (i.e. enhanced due to the linearised approximation used) are displayed (y axis) for all mentioned profiles in dependence on the real averaged density ( $x$  axis) on the top part of Fig. 1. Surprisingly, it has been found that the form of the profile does not play any decisive role (except the non-physical triangle profile), at least for the averaged density lower than approx. one half of the critical density. Therefore we approximate the relation between  $n_{in}$  and the real density for all values of  $p$  between 3 (inhomogeneous plasma) and infinity (homogeneous plasma) by a single fitting curve.

In this way, we elaborated a graph, where for every density value  $n_{in}$  there are two values of the averaged densities. The smaller one corresponds to the real averaged density  $n_{real}$ . The greater one corresponds to the value  $n_{in}$ , evaluated incorrectly from the phase linear approximation. In this way, a following simple transformation formula from the erroneously “evaluated”  $n_{in}$  to the correct real averaged density  $n_{real}$ , has been obtained (again numerically):

$$n_{real} = \frac{n_{in}}{[1 + 0.9 \cdot (n_{in}/n_{crit})]} \quad (2)$$

Differences between the incorrectly evaluated (measured, neglecting non-linear effects – dashed line) electron density and the real electron density (solid line) can be seen on the bottom Fig. 1.

## 3. Real-time control

Real-time control on the COMPASS tokamak [9] is done using a real-time framework MARTE (Multi-threaded Application Real-Time executor) [10,11]. MARTE at present runs at two isolated cores at a four core CPU assembled in a motherboard placed in the ATCA (Advanced Telecommunications Computing Architecture) crate [12–14]. One CPU is used for a fast thread which is executed in a 50  $\mu\text{s}$  loop, second one is used for a slow thread which is executed in a 500  $\mu\text{s}$  loop. One of the remaining cores is dedicated to carry out the management tasks of Linux. The threads are composed of the generic application modules (GAMs), blocks of the code

that perform specific tasks. Sequence of following tasks is used for electron density control.

At the beginning of the process, output voltage from the interferometry is measured with the MARTe GAM. Then offset of the voltage is subtracted from measured signal with drift removing GAM. Afterwards, GAM for calculation of real electron density is performed. Firstly, electron density is calculated according to Eq. (1) where the length and the plasma position and the shape are taken into account. Then, the  $n_{cor}$  from Eq. (1) is used in Eq. (2) as  $n_{in}$  (i.e.  $n_{in} \equiv n_{cor}$ ) and linearisation is performed. After proper calculation of the electron density, GAM for feedback control uses proportional and integral part of a PID (Proportional–Integral–Derivative) controller to calculate requests for the valve. The PI controller controls the gas-puff valve opening and thus controls the amount of the gas inlet to the tokamak vessel as described in Section 3.1. Finally, control of the piezo-electric gas-puff valve is programmed in dedicated GAM for converting requests to the voltage.

### 3.1. Stickiness of piezo-electric valve

There are two piezoelectric valves currently installed on COMPASS, one on the low field side, other on the high field side of the torus. This gives us the opportunity to study the influence of the gas inlet location. As noted above, the electron density is controlled by controlling the amount of the injected working gas, in a feedback loop, which uses the interferometer measurement of the electron density as an input and returns requested values for the voltage to open the selected valve. Thus, either one gas-puff location can be selected or, optionally, the other valve can be (a) controlled with a pre-defined feedforward wave-form throughout the whole discharge or (b) used for experiments with gas-puff imaging. In principle, both valves can be connected to feedback control loop in future.

The piezo-electric valves may suffer from a stickiness. To suppress the stickiness of the valve and to open the valve fast, maximum voltage of 100 V has to be used for several milliseconds (usually around 5 ms) at the first opening. It is typically done using a predefined waveform for the piezo-electric valve at the beginning of the discharge (approximately 30 ms before breakdown). This fills the tokamak vessel at pressure around  $1 - 4 \times 10^{-2}$  Pa. The feedback control loop then overtakes the gas-puffing approximately 10 ms after breakdown (usually 980 ms). If the maximum voltage is applied for less than 5 ms, the valve may not open or amount of gas filled into the tokamak vessel will not be sufficient for the plasma breakdown.

Once the valve is fully opened, it can be controlled easily and fast. If the valve is fully closed during a discharge and then there is a new request to open the valve again, additional time is needed and this causes delay in control. According to characteristics of the valves, typically voltage between 30 and 50 V (i.e. 30–50% of the maximum) can be required to keep the valve open. Lower voltage, approx. 20–30 V, keeps valve closed but the feedback reaction remains fast.

### 3.2. Calibration

Piezo-electric valves can have different characteristic for the opening. Ranges of characteristics are different for every single valve, therefore calibration of our valve had to be done, before using it in real-time control loop. First, we opened valve at 100% with 100 V amplifier for a short time of 5–9 ms and measured pressure in the vacuum vessel. Fig. 2 shows that first 5 ms gas puff was smaller than two others 5 ms pulses. This was caused by stickiness at the first opening of the valve after several hours without operation.

After this measurements 6 ms long pulse was chosen, because amount of gas puffed during such pulse was suitable for plasma

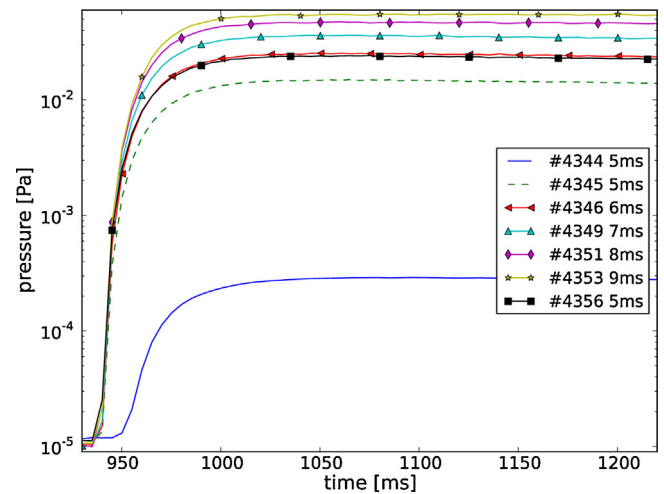


Fig. 2. Hydrogen gas-puffing for calibration of the valve. Valve was opened at maximum (100 V) at the same time for different lengths 5–9 ms.

breakdown. This 6 ms pulse was followed by 300 ms pulse with different level of opening between 10 and 50 V. The applied voltage used after first 6 ms pulse is marked in the legend of Fig. 3 after the shot number. We can see how pressure in the vessel decreases if voltage is less than 20 V. Voltage even higher than 30 V has to be used to increase pressure in the vessel. Therefore, we set lowest voltage during experiment to 20 V to keep valve closed, but not to loose its fast reactions in the feedback control.

## 4. Results

In Fig. 4 we can see different phases of feedback controlled electron density and advantages of the digital control. At the beginning of the discharge we can see controlled electron density, with feedback starting at 970 ms (first vertical black dashed line). Electron density follows predefined waveform and follows density ramp-up. Feedback on density is switched off at 1050 ms (second black dashed line) and experiment with gas puff imaging followed. During this experiment, plasma density was not controlled and high inlet of gas was used. Therefore, electron density kept rising despite the fact that the main piezo-electric valve was closed. Control

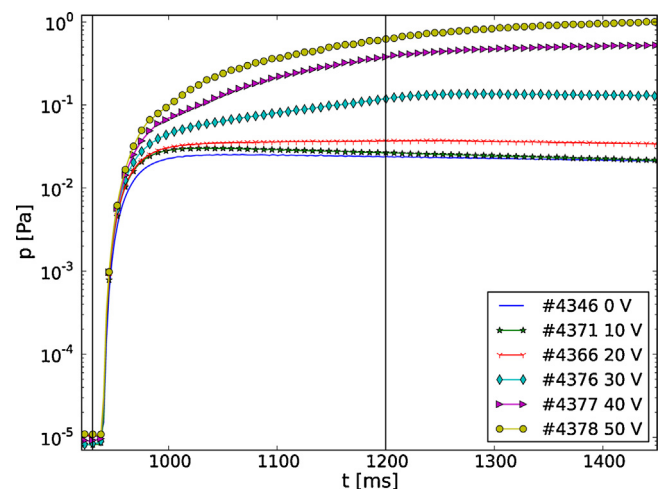
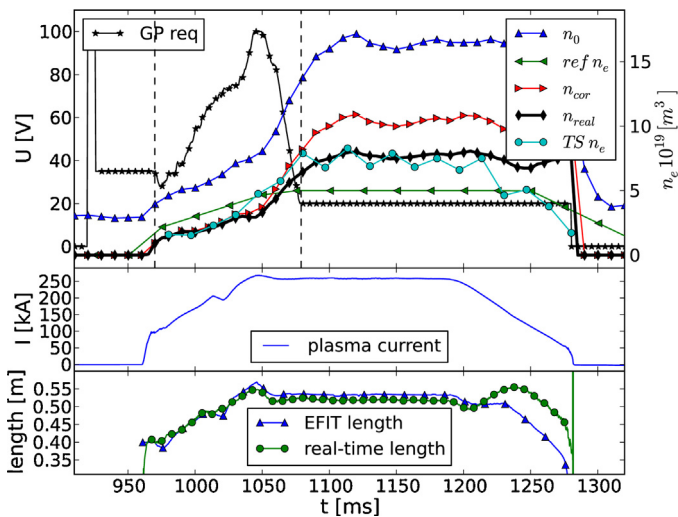


Fig. 3. Hydrogen gas-puffing for calibration of the valve. Valve was opened at 930 ms till 1200 ms for 0–50 V after 6 ms long pulse at the maximum voltage (100 V). Vertical lines show when valve was open and closed.



**Fig. 4.** Top graph: The measured  $n_0$ , corrected  $n_{cor}$ , requested density  $ref n_e$  and density from Thomson Scattering diagnostic  $TS n_e$  and the output signal of the feedback system from the gas puff valve – GP req. The black dashed vertical lines show time interval when the feedback control was used. Middle graph: The plasma current during the discharge. Bottom graph: Comparison between chord length calculated in real-time according to Eq. (1) and EFIT reconstruction after the discharge.

output from real-time calculation for the valve opening (analogue request) is shown in the top of the figure. Measured plasma current is in the middle of the figure.

The bottom part of Fig. 4 shows length of plasma calculated on  $R=0.56$  m in real time and comparison with EFIT reconstructed length of plasma at the same position. We can see nice agreement with difference less than 5%.

## 5. Conclusion

Controlling of electron density is necessary for investigation of the plasma physics in tokamaks. Newer precise calculation of interferometer chord length and non-linearity was introduced, which give us chance to control electron density more accurately. Better calculated density in real-time is essential for parametric scans for diagnosticians and for physics experiments. Also H-mode could be achieved only with feedback controlled density [3]. Also the measured electron density from the interferometer is in very good

agreement with measurement from the Thomson scattering measurement.

## Acknowledgements

The work at the Institute of Plasma Physics AS CR, v.v.i. was supported by project MSM12011021. This project has received funding from the European Union's Horizon 2020 research and innovation programme under grant agreement number 633053. The views and opinions expressed herein do not necessarily reflect those of the European Commission.

## References

- [1] R. Panek, O. Bilykova, V. Fuchs, M. Hron, P. Chraska, P. Pavlo, et al., Reinstallation of the COMPASS-D tokamak in IPP ASCR, Czechoslov. J. Phys. 56 (2006) B125–B137.
- [2] P. Deichuli, V. Davydenko, V. Belov, A. Gorbovsky, A. Dranichnikov, A. Ivanov, et al., Commissioning of heating neutral beams for COMPASS-D tokamak, Rev. Sci. Instrum. 83 (2012) 02B114.
- [3] R. Panek, J. Stockel, J. Havlicek, F. Janky, M. Hron, V. Weinzettl, et al., Characterization of ohmic and NBI heated H-mode in the COMPASS tokamak, in: EPS Conference on Plasma Physics, 2013, pp. 1–4 (Papers), P4.103.
- [4] V. Weinzettl, R. Panek, M. Hron, J. Stockel, F. Zacek, J. Havlicek, et al., Overview of the COMPASS diagnostics, Fusion Eng. Des. 86 (2011) 1227–1231.
- [5] M. Varavin, J. Zajac, F. Zacek, S. Nanobashvili, G.P. Ermak, A.V. Varavin, et al., New design of microwave interferometer for tokamak COMPASS, Telecommun. Radio Eng. 73 (2014) 571–575.
- [6] J. Urban, J. Pipek, M. Hron, F. Janky, R. Paprok, M. Peterka, et al., Integrated data acquisition, storage, retrieval and processing using the COMPASS DataBase (CDB), Fusion Eng. Des. 89 (2014) 712–716.
- [7] F. Janky, J. Havlicek, A. Batista, O. Kudlacek, J. Seidl, A. Neto, et al., Upgrade of the COMPASS tokamak real-time control system, Fusion Eng. Des. 89 (2014) 186–194.
- [8] F. Janky, J. Havlicek, D. Valcarcel, M. Hron, J. Horacek, O. Kudlacek, et al., Determination of the plasma position for its real-time control in the COMPASS tokamak, Fusion Eng. Des. 86 (2011) 1120–1124.
- [9] M. Hron, F. Janky, J. Pipek, J. Sousa, B. Carvalho, H. Fernandes, et al., Overview of the COMPASS CODAC system, Fusion Eng. Des. 89 (2014) 177–185.
- [10] A.C. Neto, F. Sartori, F. Piccolo, R. Vitelli, G. De Tommasi, L. Zabeo, et al., EFDA/JET contributors, MARTE: a multiplatform real-time framework, IEEE Trans. Nucl. Sci. 57 (2010) 479–486.
- [11] A. Neto, D. Alves, L. Boncagni, P. Carvalho, D. Valcarcel, A. Barbalace, et al., A survey of recent MARTE based systems, IEEE Trans. Nucl. Sci. 58 (2011) 1482–1489.
- [12] D.F. Valcarcel, A. Neto, J. Sousa, B.B. Carvalho, H. Fernandes, J.C. Fortunato, et al., An ATCA embedded data acquisition and control system for the COMPASS tokamak, Fusion Eng. Des. 84 (2009) 1901–1904.
- [13] D.F. Valcarcel, A.S. Duarte, A. Neto, I.S. Carvalho, B.B. Carvalho, H. Fernandes, et al., Real-time software for the COMPASS tokamak plasma control, Fusion Eng. Des. 85 (2010) 470–473.
- [14] D.F. Valcarcel, A. Neto, I.S. Carvalho, B.B. Carvalho, H. Fernandes, J. Sousa, et al., The COMPASS tokamak plasma control software performance, IEEE Trans. Nucl. Sci. 58 (2010) 1490–1496.